Brightly Luminescent Organically Capped Silicon Nanocrystals Fabricated at Room Temperature and Atmospheric Pressure

Kateřina Kůsová,[†,*] Ondřej Cibulka,[†] Kateřina Dohnalová,[†,¶] Ivan Pelant,[†] Jan Valenta,[‡] Anna Fučíková,[†,‡] Karel Žídek,[†,‡] Jan Lang,[‡] Jiří Englich,[‡] Pavel Matějka,[§] Petr Štěpánek,[∥] and Snejana Bakardjieva[⊥]

[†]Institute of Physics of the ASCR, v.v.i., Cukrovarnická 10, 162 53 Prague 6, Czech Republic, [‡]Faculty of Mathematics and Physics, Charles University, Ke Karlovu 3, 121 16 Prague 2, Czech Republic, [§]Institute of Chemical Technology, Technická 5, 166 28 Prague 6, Czech Republic, [∥]Institute of Macromolecular Chemistry of the ASCR, v.v.i., Heyrovského náměstí 2, 162 06 Prague 6, Czech Republic, and [⊥]Institute of Inorganic Chemistry of the ASCR, v.v.i., 250 68 Řež, Czech Republic. [¶]Current address: van der Waals-Zeeman Institute for Experimental Physics, University of Amsterdam, Valckenierstraat 65, 1018 XE Amsterdam, The Netherlands.

ABSTRACT Silicon nanocrystals are an extensively studied light-emitting material due to their inherent biocompatibility and compatibility with silicon-based technology. Although they might seem to fall behind their rival, namely, direct band gap based semiconductor nanocrystals, when it comes to the emission of light, room for improvement still lies in the exploitation of various surface passivations. In this paper, we report on an original way, taking place at room temperature and ambient pressure, to replace the silicon oxide shell of luminescent Si nanocrystals with capping involving organic residues. The modification of surface passivation is evidenced by both Fourier transform infrared spectroscopy and nuclear magnetic resonance measurements. In addition, single-nanocrystal spectroscopy reveals the occurrence of a systematic fine structure in the emission single spectra, which is connected with an intrinsic property of small nanocrystals since a very similar structure has recently been observed in specially passivated semiconductor CdZnSe nanoparticles. The organic capping also dramatically changes optical properties of Si nanocrystals (resulting ensemble photoluminescence quantum efficiency 20%, does not deteriorate, radiative lifetime 10 ns at 550 nm at room temperature). Optically clear colloidal dispersion of these nanocrystals thus exhibits properties fully comparable with direct band gap semiconductor nanoparticles.

KEYWORDS: silicon nanocrystals · organic capping · photoluminescence · NMR · single-nanocrystal spectroscopy

Luminescent silicon nanocrystals (Si-nc) have been extensively studied in recent years with an outlook for various applications ranging from solid-state light-emitting devices[1,2] through fluorescent biological labels[3] to chemical sensing.[4,5] In this material, whose typical sizes are on the nanometer scale, the surface-to-volume ratio substantially increases and thus the interface between the Si-ncs and their environment plays a crucial role in tailoring their optical properties. In principle, two different approaches are being used to affect the surface chemistry of Si-nc. The first one (more frequently used by physicists) consists of treating Si-ncs as a solid sample, for example, by embedding the Si-nc into a solid matrix, usually silicon dioxide.[6−10] The surface passivation in this case is believed to be due to either a Si═O double bond[7] or a Si−O−Si bridge bond.[11,12]

The second pathway then takes advantage of a more versatile possibility of modifying the surface morphology of Si-nc in a liquid[13] (colloidal suspension or dispersion) or even in a gas state; these procedures are used predominantly by chemists. A large family of organic molecules, mainly the derivatives of various alkenes,[14−17] and also alkyl[18,19] or other[20,21] chains can be grafted to the surface of Si-nc, resulting in the Si−C surface-bond capping. During the preparation, the oxidation of Si-nc is always avoided in order to deal with a primary fresh hydrogen-passivated silicon surface.

As for the efficient Si-ncs' luminescence, in contrast to their bulk counterpart, it is thought to be caused by several processes, depending on both the size and surface. First, the spatial localization of an electron−hole pair in a nanometer-sized nanocrystal increases the uncertainty of their crystal momentum, resulting in the occurrence of quasi-direct transitions.[22] When the band gap gets large enough, surface states set in[23] and start to considerably suppress further photoluminescence (PL) shift. Especially when the surface states are SiO_2-related, it seems to be impossible to shift the Si-ncs' PL into the yellow and green region, with the borderline wavelength being at ∼590 nm.[24] As Si-ncs are strongly prone

*Address correspondence to kusova@fzu.cz.

Received for review March 12, 2010 and accepted July 26, 2010.

Published online August 6, 2010. 10.1021/nn1005182

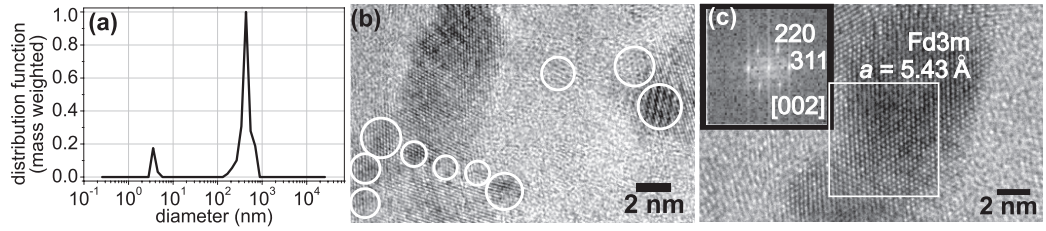

Figure 1. (a) DLS measurements of the (mass-weighted) distribution function of particles' sizes in the colloid (sample was dispersed in the original solvent, 220 nm pore size filtration was applied). (b) HRTEM measurements confirm the presence of small (2−3 nm) nanocrystals, which are circled for easier orientation. The electron diffraction pattern in the inset of (c) of a slightly larger nanocrystal shown in the figure is characteristic of silicon.

to oxidation in normal atmosphere,[4] Si-ncs commonly exhibit oxide surface state related PL decay in the microsecond range,[25] although it is worth mentioning that nanosecond PL decay has been observed in organically capped Si-ncs.[26]

Apart from a clear distinction to core-related and surface states, a model involving the cooperation of these two has been proposed.[27]

RESULTS AND DISCUSSION

In this article, we show that it is possible, using a photochemical approach, to start with oxide-passivated Si-ncs (Si-nc:O) and prepare a colloidal dispersion of Si-ncs with a substantially altered surface layer made of organic residues, including methyl groups covalently bound to the silicon surface (Si-nc:C). This approach allows us to make a unique comparison of optical properties of Si-nc:O and Si-nc:C while keeping their crystalline core unchanged. It also shows that the alteration of the surface layer leads to a significant improvement in PL properties, putting the Si-nc:C on a par with direct band gap semiconductor nanocrystals.

Since the study of optical properties of Si-nc:O has already been published elsewhere,[25,28,29] the main focus of this article is placed on an in-depth analysis of the surface chemistry and optical properties of the Si-nc:C, including single-nanocrystal spectroscopy.

Preparation of the Si-nc:C Colloid. During the preparation process, in brief, we start with electrochemically etched Si-nc powder, that is, aggregates sized on the order of 0.1−1 μm of individual Si-nc:O with the mean size of the Si-nc crystalline core of 2.7 nm[28] (and natural oxide passivation). This powder is dispersed in a solvent (mixture of xylene isomers, ethylbenzene, and isopropylbenzene with trace amounts ~0.1% of di/trimethylcyclohexane). The suspension of Si-nc and the solvent is kept under constant magnetic stirring and is irradiated with a cw UV laser (325 nm, 3.81 eV, 367 kJ mol^{-1}) at regular intervals. Although the exact chemical mechanism has yet to be found, the process was verified to be easily repeatable when keeping the parameters of laser irradiation (laser output, intervals between irradiation) constant. A cooperation of several different kinds of molecules may be indispensable for obtaining the Si-nc:C colloidal dispersion. Although the more complicated mixture of solvents helps us obtain the final product more easily, it also, on the other hand, makes it more difficult to identify the reaction mechanism.

During this mechano-photochemical treatment, the original PL band (the so-called S-band, peaking at ~600−650 nm, depending on the "type" of used Si-nc:O powder[28]) fades away and a new yellow one, clearly boosted by the UV irradiation, appears. The process is not abrupt; that is, the orange PL band is gradually replaced by the yellow one rather than undergoing a continuous blue shift (see Supporting Information for more details). The resulting Si-nc:C-based colloid is obtained by filtrating the supernatant of the irradiated suspension. The whole procedure intentionally takes place at room temperature and normal pressure and atmosphere, in view of practical application. Unlike many colloids prepared from hydrogen-passivated Si-ncs, our sample is stable in the long term (for about 3 years now) and the colloid does not further precipitate (*i.e.*, it remains optically clear).

DLS and HRTEM Characterization. First, we focused on confirming the presence of Si-nc in the filtered colloid. Dynamic light scattering (DLS) measurements in Figure 1a revealed the presence of two main sizes of particles in the colloid. While the larger particles (200−300 nm) probably represent the agglomerates of the precursor nanocrystals persisting in the colloid even after the filtration procedure (filter with pore diameter of 220 nm was used), small particles with sizes of individual nanocrystals clearly crumbled away from these larger agglomerates. Their size as determined from DLS (3.4 nm in diameter including the surface) agrees reasonably with previous estimates of the size of the precursor Si-nc:O (2.7 nm Si core;[28] for number of particles weighted distribution, see Supporting Information).

Second, high-resolution transmission electron microscopy (HRTEM) measurements confirmed that the small particles are crystalline (Figure 1b), similar to the precursor nanocrystals.[28] Moreover, the electron diffraction of a larger nanocrystal (Figure 1c) is characteristic of silicon, and the FFT transform obtained from it (the marked area in Figure 1c) can be indexed on the basis of a cubic type cell with space group *Fd*3*m* and

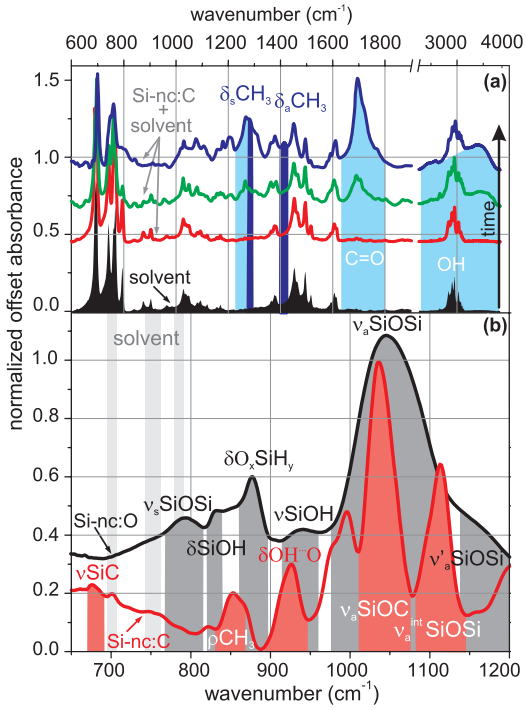

Figure 2. (a) FTIR-ATR spectra of the original solvent (black shaded area) and Si-ncs:C colloid (red, green, and blue curves) during the evaporation of volatile components. Features emerging after the irradiation procedure are shaded in blue for easier orientation. The bottom-most spectrum represents the very first acquisition, while the top-most is the very last one; that is, the degree of the evaporation of the solvent rises from the bottom upward. Measurements were carried out with Si-ncs being dispersed in the original solvent, and no filtration was applied. FTIR-ATR spectra in (b) show a zoomed-in region of 650−1200 cm^{-1} of the Si-nc:O precursor (black) and the Si-nc:C colloid dispersed in ethanol and filtered using a 10 nm nominal pore size fiter (in red) (bands shaded in light gray are probably due to traces of the original solvent).

(silicon) lattice parameter $a = 5.43$ Å. These observations unambiguously prove that small Si-ncs are present in our colloid.

Surface Chemistry Analysis: FTIR and NMR Characterization. The differences between the compositions of the surface layers of treated and untreated Si-ncs were studied using Fourier transform infrared absorption measurements in attenuated total reflection mode (FTIR-ATR). In the first series of measurements, where the Si-ncs:C were still dispersed in the original solvent and no filtration was applied, the IR absorbance of a droplet of the colloidal dispersion was measured at various time delays elapsed after putting the droplet onto the measuring internal reflection element. It is evident that when the droplet gets more concentrated due to the progressing evaporation of the solvent new pronounced absorption bands appear (Figure 2a). The most prominent ones (at 1700 and 2400−3600 cm^{-1}, see Table 1 for assignments) show that the solvent molecules underwent oxidation in their alkyl groups to corresponding aldehydes and carboxylic acids.

TABLE 1. Assignment of FTIR Vibrations Observed in This Work (ν stretching, δ deformation, ρ rocking mode, a antisymmetric, s symmetric)[a]

functional group	mode	frequency (cm^{-1})	ref
carboxylic acids	ν O−H	∼2400 −3600	30
	ν C═O	1693	30
−COOH (dimer)	ν C−O	1265	30
	δ O−H···O	926	30
$SiCH_3$	δ_a CH_3	1415	30, 31
	δ_s CH_3	1280	30, 31
	ρ Si−CH_3	852	30, 31
	ν Si−C	677	31, 32
SiOSi	ν_a Si−O−Si	∼975 −1130	33−35
	ν'_a Si−O−Si	∼1130 − 1260*	33, 35
	ν_s Si−O−Si	∼795	33, 34
OSiH	ν O_x−SiH_y	2262	34, 35
	δ O_x−SiH_y	875	34, 35
SiOH	ν Si−OH	∼940	36
	δ Si−OH	833	36
SiOC	ν Si−O−C	1040	30, 32
SiOSi	ν_a^{int} Si−O−Si	1111#	35, 37, 38

[a]Shoulder peak (*) corresponds to 180° out-of-plane motion of the oxygen atoms; # this vibration comes from interstitial oxygen inside Si-ncs, which are electrochemically prepared from Czochralski-grown Si wafers).

Peaks that are of main interest here, however, are those possibly connected with Si−CH_3 vibrations at 1280 and 1415 cm^{-1} (see Table 1 and also Figure S4 for more detailed FTIR spectra). Unfortunately, the crucial Si−C region of 600−800 cm^{-1} is obscured by the intense aromatic out-of-plane CH deformation vibrations of the original solvent. To overcome this setback, the original solvent was left to evaporate and the Si-ncs:C were dispersed in ethanol and filtered with an ultrafine filtration unit (100 kDa, nominal pore size of 10 nm). FTIR-ATR spectrum of the ethanol-based colloidal dispersion in Figure 2b (red curve) then reveals the remaining Si−CH_3 mode (852 cm^{-1}) together with the Si−C stretch[31] at 677 cm^{-1} (although this band seems to be quite weak, it is important to point out that the useful range of our FTIR-ATR spectrometer ends at ∼650 cm^{-1}). The presence of this band in the FTIR spectra indicates that at least part of the methyl groups are attached directly to the silicon surface, while the surface layer of the Si-nc:O precursor (see black curve in Figure 2b) is made up of silicon oxide (evidenced by Si−O−Si stretches between 975 and 1260 and at 795 cm^{-1}) with the incorporation of some hydrogen atoms (silanol Si−OH groups and oxidized hydride groups O_x−SiH_y at ∼940, 875, and 833 cm^{-1}; 2262 cm^{-1} vibration is not shown), which are expected in oxidized Si-ncs.[35]

The comparison of the oxide-related FTIR spectral region of Si-nc:O and Si-nc:C between 975 and 1250 cm^{-1} together with the disappearance of the 795 cm^{-1} band point to a significant chemical change of the initial oxide layer occurring after the irradiation procedure is applied and further after filtration (see Figure S4 in the Supporting Information). The correlation between the

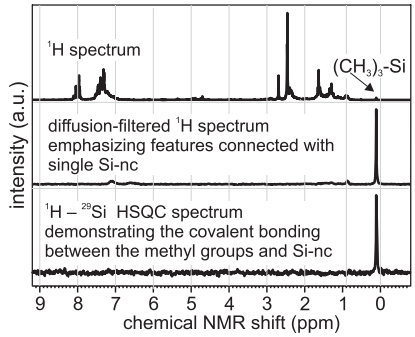

Figure 3. Acquired key NMR spectra demonstrate methyl capping of several-nanometer-sized silicon particles (the organically capped silicon nanocrystals are dispersed in chloroform); see text for details.

suppression of the oxide-related bands and the filtration procedure indicates that larger agglomerates of sizes of the order of ~100 nm are oxide covered, while the small single nanocrystals which crumble away from the agglomerates (as evidenced by DLS) have different surface chemistry.

However, a new band at 1040 cm^{-1} appears in the spectra of the Si-nc:C colloid. Since this band is much narrower than the original silicon oxide band, we believe it to be of different origin, and tentatively assign it to Si−O−C bonds existing on the surface of the nanocrystals. Consequently, the changes in the surface layer of the Si-nc:C seem to involve also the attachment of organic molecules *via* a Si−O−C linkage.

The last band to be assigned in Figure 2b lies at 1111 cm^{-1}. This peak is known to occur in Czochralski-grown Si wafers,[37] where it is due to antisymmetric stretches of interstitial oxygen impurities in the silicon lattice. Since our Si-ncs are made of such wafers, we believe this peak to be of similar origin in our Si-nc:C, indicating, however, that this vibration is connected with the "bulk" of the Si-ncs:C and not with their surface.[39]

An independent investigation of the colloidal Si-ncs was carried out by nuclear magnetic resonance (NMR) spectroscopy, results of which are shown in Figure 3. For this measurement, the colloid was left to dry out and redispersed in deuterated chloroform ($CHCl_3$-d_1). The ^{1}H NMR spectrum (Figure 3, top) is, at the first glance, quite complex, indicating the presence of several similar species containing aliphatic as well as aromatic parts.

Diffusion NMR measurements revealed that species with two diffusion coefficients differing by about an order of magnitude are present in the colloid; while a vast majority of resonances in the ^{1}H spectrum belong to small-molecular mass species (the diffusion coefficient of about 1100 $\mu m^2/s$), a significantly lower diffusion coefficient (158 $\mu m^2/s$) was determined for a single peak at 0.1 ppm. The diffusion-filtered ^{1}H NMR spectrum (Figure 3, middle), emphasizing the larger species with slower diffusion, demonstrates that all resonances except for the one at 0.1 ppm are suppressed by fast translational diffusion. A simple application of the Stokes−Einstein equation, giving a rough estimate of the particle's size, yields the hydrodynamic diameter of the particle corresponding to the lower diffusion coefficient of ~5 nm (using the dynamic viscosity of chloroform of 0.54 mPa · s at 298 K), which reasonably agrees with the previously mentioned HRTEM and DLS measurements of the size of single Si-ncs in the colloid. Consequently, this single ^{1}H resonance (0.1 ppm) is directly correlated with nanometer-sized particles by NMR.

Moreover, two-dimensional ^{1}H−^{29}Si heteronuclear single quantum coherence (HSQC) spectrum (see Supporting Information) unambiguously proves that this hydrogen is located in the distance of 2 or 3 chemical bonds from the silicon atom resonating at −43 ppm (for ^{1}H−^{29}Si HSQC see Figure S5, one-dimensional ^{1}H−^{29}Si HSQC is shown in Figure 3, bottom). ^{1}H−^{13}C heteronuclear multiple-bond correlation (HMBC) and ^{1}H−^{13}C HSQC spectra provided a single-bond correlation of this proton resonance to carbon with a chemical shift of 1 ppm while no multiple-bond correlations were observed. Finally, the carbon resonance is split into a quartet with a one-bond indirect coupling constant $^1J_{CH}$ = 120 Hz in the ^{13}C−^{1}H INEPT spectrum. All in all, the NMR measurements provide an unequivocal assignment of the observed molecular grouping as $(CH_3)_3$Si−, firmly establishing the organic capping of Si-nc, which, in this case, admits methyl groups covalently bound to silicon.

Obviously, both FTIR and NMR measurements evidence the attachment of organic residues onto the Si-nc surface through Si−C and Si−O−C bonds.[40] Therefore, even if we cannot completely rule out the possibility that trace amounts of fluorine ions remaining in the Si-nc:O agglomerates from the electrochemical etching procedure attack the surface SiO_x similarly as in ref 41, we suggest rather that the organic residues attach to the Si-ncs by attacking the Si−O−Si bridge bonds on the surface of Si-nc, which results in both Si−O−C and Si−C bonding in the final product. The attachment of methyl radicals directly to the Si surface (*i.e.*, Si-CH_3 groups) is backed up by both FTIR and NMR. However, the radical attached through Si−O−C bonding is most probably not a methyl group because an −O−CH_n group would give rise to a signal between 3 and 5 ppm in the diffusion-filtered ^{1}H NMR spectrum in Figure 3. Similarly, signal from hydrogen chemically bonded to silicon over up to three chemical bonds (*i.e.*, Si−O−CH_3) should appear in the ^{1}H−^{29}Si HSQC NMR spectrum in Figure S5 (Supporting Information), which is again not the case. The carbon in the Si−O−R groups is therefore probably quaternary, that is, with no hydrogen atoms attached to it. Although it is possible to think of several chemical groups which are not contradictory to the NMR measurements (*e.g.*, Si−O aromatic,

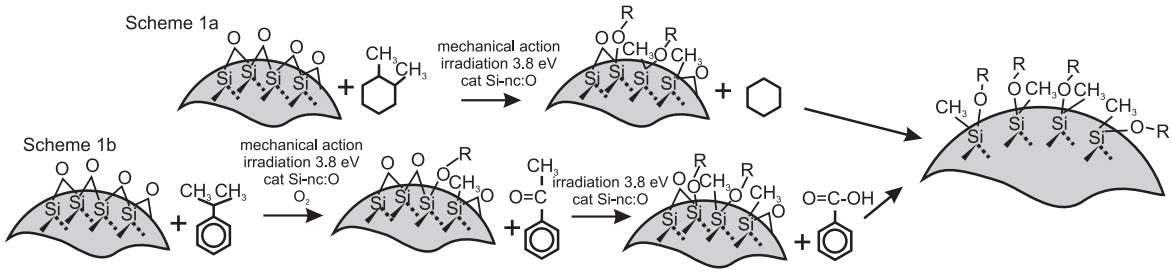

Scheme 1. Proposed Mechanisms of Breaking of the Si−O−Si Bridge Bonds

Si−O−(C═O)−R′, *etc.*), we are currently unable to identify the Si−O−R with a concrete chemical group.

More sources of photodissociated methyl radicals attacking the Si−O−Si bridges can be present, and two possibilities are proposed in Scheme 1. First, methyl radicals can be generated *via* the photodissociation of alkyl-substituted cyclohexane (Scheme 1a) (a decrease in the amount of dimethylcyclohexane accompanied by the appearance of cyclohexane is evidenced by liquid chromatography measurements of the solvent and the final product; bond dissociation energy of a methyl radical from methylcyclohexane[42] is 377 kJ/mol ≈ 3.9 eV). As one methyl radical attacks the Si−O−Si bond, a dangling bond is left on the Si-nc's surface, which may in turn induce further photodissociation similarly as proposed in the article by Linford *et al.*[43] In fact, the photodissociation generating the methyl radicals might also be initiated by the creation of dangling bonds *via* the abstraction of hydrogen from the oxidized surface hydride groups $-O_x-SiH_y$ in the presence of UV irradiation; on hydrogenated silicon surfaces, the minimal energy needed for the homolysis of the Si−H bond[38] is 3.5 eV (*i.e.*, 338 kJ mol^{-1} or 350 nm irradiation, although $-O_x-SiH_y$ groups are stronger than simple Si−H bonds.[35]) A possible second source of methyl radicals might lie in the autoxidation of isopropylbenzene to acetophenone consuming atmospheric oxygen dissolved in the solvent and further to the benzoic acid (Scheme 1b).[44−46]

Ensemble Photoluminescence Properties. Even though the Si-ncs' core remains more or less unchanged by the treatment in the colloid, optical properties of Si-nc in the precursor and in the colloid vary substantially (Figure 4): the original PL, whose dominant feature is an orange S-band, blue shifts to the yellow spectral region (640 → 570 nm) and the PL decay shortens by about 4 orders of magnitude (23 μs → 2 ns; *i.e.*, the PL of Si-ncs:C contains no slow component whatsoever). Moreover, the PL quantum efficiency rises about 10-fold (from 2−3% for Si-nc:O to 20% for Si-nc:C). This striking difference in PL and its dynamics can be easily understood and fully corroborates the observed alteration of the surface oxide layer of Si-ncs: the slow orange PL in Si-ncs:O is well-known to be due to ultrafast trapping to and subsequent slow decay from oxide-related surface states,[25,47] whose chemical alteration must lead to the disappearance of the slow PL at 640 nm and gives way to alternative recombination channels.

Since both the PL lifetime τ_{PL} and the quantum efficiency η were acquired, it is possible to directly calculate the radiative lifetime ($\tau_r = \tau_{PL}/\eta$) of our Si-nc:C. Its value of as little as 10 ns makes the presented colloidal Si-nc:C comparable in PL performance with direct band gap nanocrystals such as CdSe.

Additional immensely important byproduct of the chemical modification of the Si-nc's surface oxide is the production of a colloidal dispersion containing single nanosized particles (as evidenced by DLS). Si-ncs:O are generally heavily prone to aggregation irreversible by ultrasonication treatment,[20] which inevitably causes large micrometer-sized aggregates to be present. These large aggregates induce light scattering of the emitted PL and thus cause the deterioration of PL performance since light-scattering-related losses can significantly hold back the onset of optical gain, an important prerequisite for applications. Thus, the combination of efficient PL and high optical quality of the sample is highly advantageous.

Last but not least, the colloidal Si-ncs:C proved to be remarkably stable in ambient conditions (for about 3 years now). The yellow PL of the Si-ncs:C was not ob-

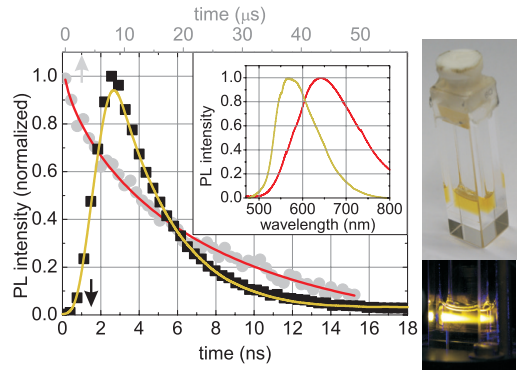

Figure 4. Comparison of basic optical properties of the colloid and Si-nc precursor. Whereas the PL dynamics (scatter plots are measured data, curves represent fits) of the colloid takes place on a nanosecond time scale (black squares, bottom axis, single exponential τ_{PL} = 2 ns), the precursor Si-nc's PL decays stretched exponentially in microseconds (gray circles, top axis, τ_{PL} = 23 μs, β = 0.77). The time-integrated PL emission spectra of the colloid (yellow curve) and the oxide-passivated Si-nc precursor (red curve) are shown in the inset, while the photos on the right demonstrate the optically clear dispersion under ambient light (top) and its bright yellow PL (excited with a 442 nm HeCd laser).

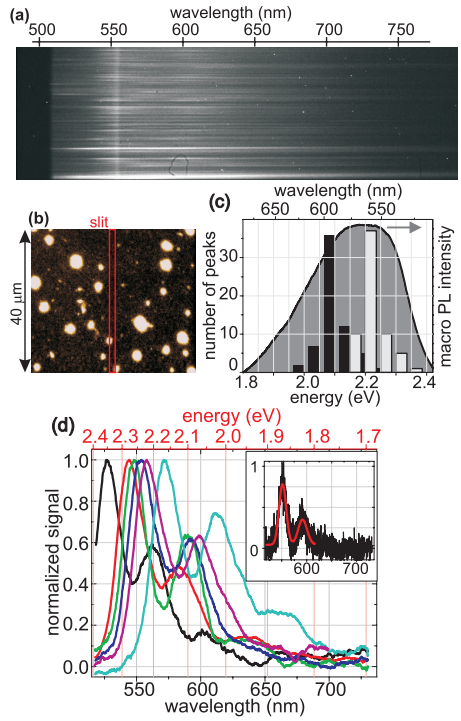

Figure 5. PL spectra of single Si-nc:C. (a) Image of single spectra and several agglomerates on the CCD (20 min acquisition). (b) PL of Si-nc as seen through the eyepiece of the optical microscope (2 min acquisition); the red rectangle denotes the position of the slit for the acquisition of spectra in (a). (d) Selected smoothed spectra of different single nanocrystals and one raw spectrum fitted with two Gaussians in the inset. The histogram of the positions of the two peaks (centers of Gaussian fits) is compared with macroscopically measured PL (gray area, redrawn from Figure 4) in (c).

served to deteriorate in the original solvent and was preserved even after the volatile components of the solvent had evaporated (under diaphragm-pump vacuum), and the Si-ncs:C were redispersed in chloroform or ethanol. Yellow luminescence was observed even in the dried-out state, even though it needs to be investigated in more detail.

Single-Nanocrystal Spectroscopy. The ultimate tool for studying optical properties of nanocrystals is single-nanocrystal (1-nc) spectroscopy. We performed these measurements on a diluted dispersion of the Si-nc:C colloid, and their results are shown in Figure 5. When a droplet of the Si-nc:C-based colloid is deposited onto the measuring prism, some nanocrystals tend to aggregate, as can be seen from Figure 5b, in which large bumps luminescing in the yellow region (when excited with an evanescent field of a laser beam of 458 nm) are shown. However, apart from these bumps, many single nanocrystals can be found between them, which is evident from the CCD image of the PL spectra measured in the area of the slit (Figure 5a). Besides, Figure 5a suggests a double-peak structure of the 1-nc spectra that becomes obvious when they are plotted *versus* wavelength (Figure 5d). The separation of these two peaks, which were observed in *all* the measured spectra, is quite strictly limited to 150 meV (150 ± 14 meV being

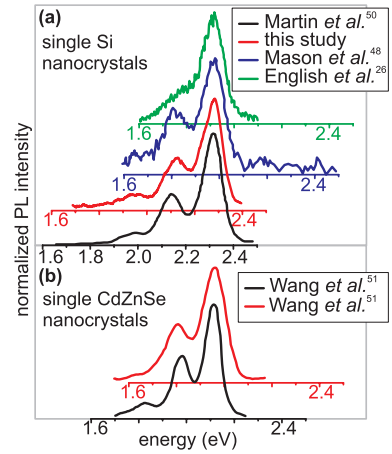

Figure 6. Comparison of 1-nc spectra of Si-ncs (a) and specially capped CdZnSe nanocrystals (b) by different groups (spectra are shifted for clarity, but all of the *x*-axes have the same scale).

the arithmetic average and standard deviation of 63 measured spectra), which strongly indicates that these two PL peaks are emitted by a single object. As for the PL characteristics, the full width at half-maximum of the first peak is approximately 100 meV and the two peaks shift between 525−575 and 560−620 nm, respectively. Most spectra have the first peak at 550−560 nm and the peak positions follow a clear Gaussian distribution (Figure 5c). Moreover, the same Figure 5c shows that the 1-nc PL spectra overlap very reasonably with the macroscopically measured PL, suggesting that the micro- and macroscopically measured spectra share a common origin.

The narrow widths and the spectral shift of the measured PL spectra are a clear fingerprint of 1-nc emission. Furthermore, these essential features very reasonably agree with earlier reports on 1-nc spectroscopy in Si-nc,[26,29,48−50] which further confirms that the origin of the observed PL lies in nanocrystals.

An interesting feature of the observed 1-nc spectra is the double-peak structure. When observed by other groups,[52] the double-peak structure was almost identical to ours[48,50] (high energy line width of about 100 meV, low-energy side satellites separated by 140−160 meV; see Figure 6a).[53] In these studies,[48,50] the 150 meV energy splitting was attributed to Si−O−Si-related vibrations, based on the fact that these vibrations can be observed with FTIR in the region between 1100 and 1400 cm^{-1} corresponding to 150 meV. However, our results throw doubt on this conclusion for several reasons. First, the treated colloidal Si-ncs:C in the present study clearly exhibit suppression of the Si−O−Si vibrations in our FTIR spectra when compared to the untreated Si-ncs:O, on which 1-nc spectroscopy measurements were also carried out[29] by our group and no double-peak structure was observed. Consequently, the correlation between Si−O-related vibrations and the double-peak structure is highly improbable. Second, the Si−O−Si vibrations appear in our FTIR spec-

TABLE 2. Description of Samples from Figure 6, Prepared and Studied by Different Groups

group	preparation and characterization of samples
Martin *et al.*[50]	pyrolysis of SiH_4, Si-ncs with oxidized surface, dispersed in toluene + PMMA
this study	electrochemically etched, Si-ncs with photochemically altered organic surface capping
Mason *et al.*[48]	electrochemical etching yielding porous Si, oxidized surface
English *et al.*[26]	arrested precipitation, Si-ncs with octanethiol capping, dispersed in chloroform
Wang *et al.*[51]	graded alloy core−shell CdZnSe/ZnSe

tra of the Si-nc:O precursor at 1060 cm^{-1} (130 meV), while the energy splitting is both in the presented and previous studies close to 150 meV (1210 cm^{-1}).[54] Third, another 1-nc PL spectra of Si-nc:C measured by English *et al.*[26] are strongly asymmetric, giving a clear indication of an unresolved second peak with a similar energy spacing (see Figure 6a, green curve). Obviously, the 150 meV energy-split structure has been observed in 1-nc PL spectra with both oxide (by Mason *et al.*[48] and Martin *et al.*[50]) and organic (by English *et al.*[26] and in the present study) passivation.

The striking similarities in both the double-peak structure and the overall shape of the 1-nc PL spectra of Si-nc samples with completely different origins (see Table 2) suggest that, down on the quantum level, unifying features take over differences due to preparation conditions. If we discard Si−O−Si vibrations as the origin of the energy splitting, other candidates are difficult to find since 150 meV lies far beyond any phonon energies in silicon.

Surprisingly, similarities of 1-nc PL spectra do not stop at differently prepared Si-ncs. A recent observation of a triple-peak structure in 1-nc spectra of specially capped[55] CdZnSe nanocrystals[51] (Figure 6b, energy splitting 164 meV) thus provides clues as to the physical origin of the energy splitting. The authors suggest that the energy splitting is connected with the occurrence of trions (a quasi-particle formed by an electron and two holes) and their radiative decay. In this case, the spectral energy splitting is driven by the energy separation of quantized hole levels.[51] Recent theoretical calculations[56] show that the energy difference of the quantized hole levels in Si-nc is also in a 100 meV range and even that the shift of the levels due to varying size does not significantly influence the energy difference, suggesting that the hole−energy separation can keep its more or less constant value even in differently sized Si-ncs, which exactly is what Figure 6a implies. Consequently, we ascribe the fine structure observed in 1-nc spectroscopy in our Si-nc:C to the quantization of hole levels in Si-ncs. We also suggest that the fine structure observed in previous studies by other authors[26,48,50] is of similar origin, based on the practically identical shape of 1-nc PL spectra.

Implications for the Origin of Photoluminescence. On the basis of our measurements, final conclusions on the origin of PL in our Si-nc:C cannot be drawn. Although the 1-nc spectroscopy measurements indicate that the intrinsic properties of the nanocrystalline core play an important role, the effect of the surface and/or interface cannot be ruled out.

Sykora *et al.*[57] experimentally demonstrated a monotonous decrease of radiative lifetime in Si-ncs as a function of confinement energy (*i.e.*, core PL emission wavelength) from $\tau_r \approx 1$ ms at $\lambda_{em} \approx 930$ nm to $\tau_r \approx 300$ ns at $\lambda_{em} \approx 530$ nm. Extrapolation of this dependence to our case ($\tau_r = 10$ ns) would yield an emission wavelength of 460 nm, far from the observed value ($\lambda_{em} = 570$ nm). The validity of such extrapolation might be questionable, however, as such a short PL wavelength ($\lambda_{em} = 460$ nm) is inaccessible through mere shrinkage of Si-nc's size[21,24] and, in addition to that, neither was such monotonous dependence observed in another type of Si-ncs:C with fast PL lifetime, as reported by English *et al.*[26] ($\tau_r \approx 100$ ns, $\lambda_{em} = 520-680$ nm).

This strongly indicates that a novel, nonconventional mechanism governed very probably by an interaction between the surface/interface and core states occurs in Si-ncs and lies behind at least the fast PL emission reported by English *et al.*[26] and in the present work. Its origin is to be specified in future research.

CONCLUSIONS

In conclusion, we showed that the initial oxide surface passivation of Si-nc can be modified by capping involving methyl groups in a xylene-based suspension *via* a photochemical reaction. The technological procedure is simple and can be realized at room temperature and ambient air pressure. Chemical changes in the suspension were studied using both FTIR-ATR and NMR, firmly evidencing attachment of organic residues on the silicon surface of nanocrystals *via* both Si−C and Si−O−C bonds. The resulting colloidal dispersion is optically clear and with long-term stability (at least 3 years). It exhibits bright PL peaking at 570 nm, with relatively high quantum efficiency of ~20% and short radiative lifetime (10 ns), proving that surface termination can play a major role not only in the passivation of nonradiative channels of recombination but also in enhancing the radiative recombination rate. The optical characteristics of the presented colloidal Si-nc:C

make this material comparable with direct band gap semiconductor nanocrystals, such as CdSe.

Moreover, the single-nanocrystal spectroscopy measurements revealed the systematic occurrence of a double-peak structure in room-temperature single-nanocrystal PL spectra, which was attributed to surface oxide vibrations in previous studies by several authors. Our results strongly indicate, however, that the observed 150 meV splitting is related to the intrinsic properties of a sufficiently small silicon nanocrystal. Most probably, the observed energy splitting is connected directly to the splitting of energy levels in a core of a quantum-confined nanocrystal.

METHODS

Preparation of the Colloid. The electrochemical etching of p-type monocrystalline wafers (B-doped, (0.075−0.100) Ωcm, (100)-oriented, etched area ~10 cm^2) yielding the Si-nc powder took place in a mixture of 50% HF and pure (>99.9%) ethanol (both from Penta) in the ratio of 1:2.5 with the current density of 2.5 mA/cm^2. (In some cases, an additional treatment of the etched wafers in H_2O_2 was applied,[28] however, without a noticeable effect on the resulting PL properties of the Si-nc:C-based colloid; see Supporting Information.) The resulting porous Si was mechanically separated off the substrate and underwent multiple sedimentations in ethanol to obtain fine powder with only small clusters. A typical starting concentration for the preparation of the colloid amounts to several milligrams of the Si-nc powder in 1 cm^3 of a mixture of aromatic hydrocarbons (which contains xylene isomers (9, 37, and 12 mol % of *o*-, *m*-, *p*-isomers, respectively), ethylbenzene (28 mol %), and isopropylbenzene (14 mol %) as determined by ^{1}H NMR and also trace amounts of (di/tri)methyl-substituted cyclohexanes as determined by liquid chromatography). After the irradiation (cw HeCd laser, 325 nm, 2.5 mW, 30 min twice a week) and stirring (600 rpm) procedure, the dispersion is filtered (using either a 220 nm Millipore Millex-GV syringe filter or a combination of Millipore Ultrafree MC centrifugal filters with pore sizes of 650 and 100 nm; in some cases, ultrafine filtration with centrifugal filters Pall Nanosep 300 and 100 kDa of nominal pore sizes as stated by the manufacturer of 35 and 10 nm, respectively, was carried out). The filtration procedure does not diminish PL intensity. As for the FTIR and NMR measurements, the samples were obtained by the evaporation of volatile components under diaphragm-pump vacuum and subsequent immersion of the product in pure ethanol (Penta, >99.9%) and chloroform-*d* (Sigma-Aldrich, 99.98 d), respectively (the ethanol-based colloid was filtered using a 100 kDa centrifugal filter).

Characterization. HRTEM image was taken with a JEOL JEM-3010 HRTEM microscope using an accelerating voltage of 300 kV; the analysis was based on PDF ICDD 27-1402 database.[58] DLS measurements were performed on a Malvern instrument Zetasizer Nano ZS equipped with a helium−neon laser; the scattering angle was 173° (mass-weighted distribution function is plotted since the larger agglomerates are not visible in the number of particle weighted distribution function; see Supporting Information), and a control solution of the solvent showed no particles. FTIR-ATR spectra were obtained with a Nicolet NEXUS 670 FTIR spectrometer; 8 μL drop was investigated, a resolution of 4 cm^{-1} and 256 scans were used. The spectra were ATR- and baseline-corrected. The absorption of ZnSe used as the ATR elements did not allow us to measure at wavenumbers under 650 cm^{-1}.

NMR spectra were acquired on a Bruker Avance 500 spectrometer working at the magnetic field of 11.7 T. In addition to the basic ^{1}H, ^{13}C, and ^{29}Si spectra, 2D ^{1}H−^{13}C HMBC, ^{1}H−^{13}C HSQC, 1D and 2D ^{1}H−^{29}Si HSQC measurements were carried out. The typical π/2 pulse lengths were 7, 13, and 12 ms for ^{1}H, ^{13}C, and ^{29}Si, respectively, in ^{1}H detected experiments and 13.4, 7.2, and 8 ms, respectively, in ^{13}C and ^{29}Si detected experiments. The pulse sequence based on the double stimulated echo[59] was utilized for the measurement of diffusion coefficients. The bipolar magnetic field *z*-gradient pulses of sine-bell shape, 2 ms duration, and 56.2 G/cm maximum amplitude were used. The total diffusion time was set at 300 ms. The diffusion-filtered ^{1}H spectrum of Si-ncs was acquired by the same pulse sequence with 4 ms bipolar gradient pulses of 45 G/cm amplitude and 200 ms diffusion time. The NMR spectra were referenced with respect to residual ^{1}H signal of chloroform-*d* (7.24 ppm) since internal tetramethyl silane had to be avoided due to its similarity with the studied Si-nc species.

Optical Measurements. All of the spectra presented in this study are corrected for the spectral response of the experimental setup. The PL decays were measured using OBB EasyLife V fluorescence system with the 450 nm LED excitation and detection at 550 nm ensured by the use of an interference filter (colloid) and a 355 nm Nd:YAG (8 ns) laser + intensified Andor CCD camera system (orange-emitting sample). The PL decay data of the colloid were fitted with a single-exponential function convoluted with the measuring system's response function, and the Si-nc precursor's PL decay data were fitted using a stretched-exponential function $I = I_0\exp\{-(t/\tau)^\beta\}$. It was verified that PL from the colloid does not contain the microsecond component using both the Nd:YAG + Andor system and a conventional spectrofluorometer. PL quantum efficiency of Si-nc:C was measured by comparing with a standard[60] (highly diluted rhodamine 6G dispersed in ethanol matching the absorption coefficient of the investigated sample) over several orders of magnitude of the excitation intensity (λ_{exc} = 480 nm of Nd:YAG + optical parametric oscillator system).

The single-nanocrystal measurements were performed using the Acton SpectraPro 2150i spectrograph with the back-illuminated CCD camera Princeton Instruments Spec-10:400B and an Olympus IX-71 microscope. A control measurement of the solvent which underwent the very same preparation procedure as the colloid (including prolonged UV laser irradiation) demonstrates that some yellow-emitting molecules are present in the solution; however, the emission is substantially weaker, and no double-peak structure was found in microscopic measurements.

Acknowledgment. This work was supported by the project IAA101120804 of the Grant Agency of the Academy of Sciences and by the Czech Ministry of Education, Youth and Sports through the research center LC510, Research Project No. 17808 of the Grant Agency of Charles University in Prague, grant KAN 400100701, and research plans MSM 0021620835 and MSM 6046137307. Research carried out in the Institute of Physics was supported by the Institutional Research Plan AV0Z10100521. We thank Zdeněk Remeš for assistance with FTIR measurements, Aliaksei Vetushka for taking the photographs of our colloidal samples, Juraj Dian for fruitful consultations, and Eva Tesařová for arranging the liquid chromatography analysis and going through the manuscript.

Supporting Information Available: More details on PL changes during the preparation procedure, detailed FTIR spectra, number of particle weighted DLS, 2D HSQC NMR, and comments on factors that may facilitate the progress of the deoxidation reaction. This material is available free of charge *via* the Internet at http://pubs.acs.org.

REFERENCES AND NOTES

1. Walters, R.; Atwater, H.; Bourianoff, G. Field-Effect Electroluminescence in Silicon Nanocrystals. *Nat. Mater.* **2005**, *4*, 143.
2. Perálvarez, M.; Carreras, P.; Barreto, J.; Morales, A.;

Domínguez, C.; Garrido, B. Efficiency and Reliability Enhancement of Silicon Nanocrystal Field-Effect Luminescence from Nitride-Oxide Gate Stacks. *Appl. Phys. Lett.* **2008**, *92*, 241104.
3. Li, Z.; Ruckenstein, E. Water-Soluble Poly(acrylic acid) Grafted Luminescent Silicon Nanoparticles and Their Use as Fluorescent Biological Staining Labels. *Nano Lett.* **2004**, *4*, 1463.
4. Sailor, M.; Lee, E. Surface Chemistry of Luminescent Silicon Nanocrystallites. *Adv. Mater.* **1997**, *9*, 783.
5. Holec, T.; Chvojka, T.; Jelínek, I.; Jindřich, J.; Němec, I.; Pelant, I.; Valenta, J.; Dian, J. Determination of Sensoric Parameters of Porous Silicon in Sensing of Organic Vapors. *Mater. Sci. Eng. C* **2002**, *19*, 251.
6. Kanemitsu, Y.; Ogawa, T.; Shiraishi, K.; Takeda, K. Visible Photoluminescence from Oxidized Si Nanometer-Sized Spheres: Exciton Confinement on a Spherical Shell. *Phys. Rev. B* **1993**, *48*, 4883.
7. Pavesi, L.; Negro, L. D.; Mazzoleni, L.; Franzò, G.; Priolo, F. Optical Gain in Silicon Nanocrystals. *Nature* **2000**, *408*, 440.
8. Linnros, J.; Lalic, N.; Galeckas, A.; Grivickas, V. Analysis of the Stretched Exponential Photoluminescence Decay from Nanometer-Sized Silicon Crystals in SiO_2. *J. Appl. Phys.* **1999**, *86*, 6128.
9. Cheylan, S.; Elliman, R. Effect of Particle Size on the Photoluminescence from Hydrogen Passivated Si Nanocrystals in SiO_2. *Appl. Phys. Lett.* **2001**, *78*, 1912.
10. Khriachtchev, L.; Navarro-Urios, D.; Pavesi, L.; Oton, C.; Capuj, N.; Novikov, S. Spectroscopy of Silica Layers Containing Si Nanocrystals: Experimental Evidence of Optical Birefringence. *J. Appl. Phys.* **2007**, *101*, 044310.
11. Kanemitsu, Y.; Shimizu, N.; Komoda, T.; Hemment, P. L. F.; Sealy, B. J. Photoluminescent Spectrum and Dynamics of Si^+-Ion-Implanted and Thermally Annealed SiO_2 Glasses. *Phys. Rev. B* **1996**, *54*, R14329.
12. Hadjisawas, G.; Kelires, P. Structure and Energetics of Si Nanocrystals Embedded in a-SiO_2. *Phys. Rev. Lett.* **2004**, *93*, 226104.
13. Wilson, W. L.; Szajowski, P. F.; Brus, L. Quantum Confinement in Size-Selected, Surface-Oxidized Silicon Nanocrystals. *Science* **1993**, *262*, 1242.
14. Hua, F.; Erogbogbo, F.; Swihart, M.; Ruckenstein, E. Organically Capped Silicon Nanoparticles with Blue Photoluminescence Prepared by Hydrosilylation Followed by Oxidation. *Langmuir* **2006**, *22*, 4363.
15. Warner, J. H.; Rubinsztein-Dunlop, H.; Tilley, R. D. Surface Morphology Dependent Photoluminescence from Colloidal Silicon Nanocrystals. *J. Phys. Chem. B* **2005**, *109*, 19064.
16. Veinot, J. Synthesis, Surface Functionalization, and Properties of Freestanding Silicon Nanocrystals. *Chem. Commun.* **2006**, *40*, 4160.
17. Stewart, M. P.; Buriak, J. M. New Approaches toward the Formation of Silicon−Carbon Bonds on Porous Silicon. *Comm. Inorg. Chem.* **2002**, *23*, 179.
18. Heintz, A. S.; Fink, M. J.; Mitchell, B. S. Mechanochemical Synthesis of Blue Luminescent Alkyl/Alkenyl-Passivated Silicon Nanoparticles. *Adv. Mater.* **2007**, *19*, 3984.
19. Chao, Y.; Šiller, L.; Krishnamurthy, S.; Coxon, P.; Bangert, U.; Gass, M.; Kjeldgaard, L.; Patole, S.; Lie, L.; O'Farrell, N.; Alsop, T.; Houlton, A.; Horrocks, B. Evaporation and Deposition of Alkyl-Capped Silicon Nanocrystals in Ultrahigh Vacuum. *Nat. Nanotechnol.* **2007**, *2*, 486.
20. Rogozhina, E.; Eckhoff, D.; Gratton, E.; Braun, P. Carboxyl Functionalization of Ultrasmall Luminescent Silicon Nanoparticles through Thermal Hydrosilylation. *J. Mater. Chem.* **2006**, *16*, 1421.
21. Sato, S.; Swihart, M. Propionic-Acid-Terminated Silicon Nanoparticles: Synthesis and Optical Characterization. *Chem. Mater.* **2006**, *18*, 4083.
22. Hybertsen, M. Absorption and Emission of Light in Nanoscale Silicon Structures. *Phys. Rev. Lett.* **1994**, *72*, 1514.
23. Wolkin, M. V.; Jorne, J.; Fauchet, P. M.; Allan, G.; Delerue, C. Electronic States and Luminescence in Porous Silicon Quantum Dots: The Role of Oxygen. *Phys. Rev. Lett.* **1999**, *82*, 197.
24. Dohnalová, K.; Ondič, L.; Kůsová, K.; Pelant, I.; Rehspringer, J. L.; Mafouana, R.-R. White-Emitting Oxidized Silicon Nanocrystals: Discontinuity in Spectral Development with Reducing Size. *J. Appl. Phys.* **2010**, *107*, 053102.
25. Dohnalová, K.; Kůsová, K.; Pelant, I. Time-Resolved Photoluminescence Spectroscopy of the Initial Oxidation Stage of Small Silicon Nanocrystals. *Appl. Phys. Lett.* **2009**, *94*, 211903.
26. English, D.; Pell, L.; Yu, Z.; Barbara, P.; Korgel, B. Size Tunable Visible Luminescence from Individual Organic Monolayer Stabilized Silicon Nanocrystal Quantum Dots. *Nano Lett.* **2002**, *2*, 681.
27. Sa'ar, A.; Reichman, Y.; Dovrat, M.; Krapf, D.; Jedrzejewski, J.; Balberg, I. Resonant Coupling between Surface Vibrations and Electronic States in Silicon Nanocrystals at the Strong Confinement Regime. *Nano Lett.* **2005**, *5*, 2443.
28. Dohnalová, K.; Pelant, I.; Kůsová, K.; Gilliot, P.; Galart, M.; Crégut, O.; Rehspringer, J.-L.; Hönerlage, B.; Ostatnický, T.; Bakardjieva, S. Closely Packed Luminescent Silicon Nanocrystals in a Distributed-Feedback Laser Cavity. *New J. Phys.* **2008**, *10*, 063014.
29. Valenta, J.; Fučíková, A.; Vácha, F.; Adamec, F.; Humpolíčková, J.; Hof, M.; Pelant, I.; Kůsová, K.; Dohnalová, K.; Linnros, J. Light-Emission Performance of Silicon Nanocrystals Deduced from Single Quantum Dot Spectroscopy. *Adv. Funct. Mater.* **2008**, *18*, 2666.
30. Socrates, G. *Infrared and Raman Characteristic Group Frequencies: Tables and Charts*, 3rd ed.; John Wiley & Sons, Ltd.: New York, 2001.
31. Canaria, C. A.; Lees, I. N.; Wun, A. W.; Miskelly, G. M.; Sailor, M. J. Characterization of the Carbon−Silicon Stretch in Methylated Porous Silicon—Observation of an Anomalous Isotope Shift in the FTIR Spectrum. *Inorg. Chem. Commun.* **2002**, *5*, 560.
32. Bateman, J. E.; Eagling, R. D.; Horrock, B. R.; Houlton, A. A Deuterium Labeling, FTIR, and *Ab Initio* Investigation of the Solution-Phase Thermal Reactions of Alcohols and Alkenes with Hydrogen-Terminated Silicon Surfaces. *J. Phys. Chem. B* **2000**, *104*, 5557.
33. Kirk, C. T. Quantitative Analysis of the Effect of Disorder-Induced Mode Coupling on Infrared Absorption in Silica. *Phys. Rev. B* **1988**, *38*, 1255.
34. Gardelis, S.; Nassiopoulou, A.; Mahdouani, M.; Bourguiga, R.; Jaziri, S. Enhancement and Red Shift of Photoluminescence of Fresh Porous Si under Prolonged Laser Irradiation or Ageing: Role of Surface Vibration Modes. *Physica E* **2009**, *41*, 986 Proceedings of the E-MRS 2008 Symposium C: Frontiers in Silicon-Based Photonics.
35. Mawhinney, D.; Glass, J. A., Jr.; Yates, J. T., Jr. FTIR Study of the Oxidation of Porous Silicon. *J. Phys. Chem. B* **1997**, *101*, 1202.
36. Burneau, A.; Carterer, C. Near Infrared and *Ab Initio* Study of the Vibrational Modes of Isolated Silanol on Silica. *Phys. Chem. Chem. Phys.* **2000**, *2*, 3217.
37. Oates, A. S.; Lin, W. Infrared Measurements of Interstitial Oxygen in Heavily Doped Silicon. *J. Cryst. Growth* **1988**, *89*, 117.
38. Hacker, C.; Anderson, K.; Richter, L.; Richter, C. Comparison of Si−O−C Interfacial Bonding of Alcohols and Aldehydes on Si(111) Formed from Dilute Solutions with Ultraviolet Irradiation. *Langmuir* **2005**, *21*, 882.
39. This band was also observed by Mawhinney *et al.*,[35] where it was proven to be connected with nonsurface oxygen by isotopic ^{18}O studies.
40. We cannot rule out the possibility of different species. If they are present in concentrations about an order of magnitude lower than the methyl groups, they are most probably below the detection limits of NMR and FTIR, considering also that their spectral features overlap with the Si-nc-unbonded molecules.
41. Boukherroub, R.; Morin, S.; Wayner, D.; Nesebaa, F.;

Sproule, G.; Baribeau, J.-M.; Lockwood, D. Ideal Passivation of Luminescent Porous Silicon by Thermal, Noncatalytic Reaction with Alkenes and Aldehydes. *Chem. Mater.* **2001**, *13*, 2002.
42. Lide, D. *CRC Handbook of Chemistry and Physics*, 88th ed.; CRC Press, Taylor & Francis: Boca Raton, FL, 2007−2008.
43. Linford, M.; Chidsey, C. Alkyl Monolayers Covalently Bonded to Silicon Surfaces. *J. Am. Chem. Soc.* **1993**, *115*, 12631.
44. This hypothesis is so far backed up only with a sizable drop in isopropylbenzene in the final product with respect to the original solvent as evidenced by NMR measurements and the presence of the products of oxidation in the FTIR-ATR spectra. The autoxidation of isopropylbenzene, however, is a well-documented process.
45. Ni, L.; Ni, J.; Lv, Y.; Yang, P.; Cao, Y. Photooxygenation of Hydrocarbons over Efficient and Reusable Decatungstate Heterogenized on Hydrophobically-Modified Mesoporous Silica. *Chem. Commun.* **2009**, 2171.
46. Sereda, G.; Rajapara, V. Benzylic Oxidation and Photooxidation by Air in the Presence of Graphite and Cyclohexene. *Tetrahedron Lett.* **2007**, *48*, 3417.
47. Guerra, R.; Degoli, E.; Ossicini, S. Size, Oxidation, and Strain in Small Si/SiO_2 Nanocrystals. *Phys. Rev. B* **2009**, *80*, 155332.
48. Mason, M. D.; Credo, G. M.; Weston, K. D.; Buratto, S. K. Luminescence of Individual Porous Si Chromophores. *Phys. Rev. Lett.* **1998**, *80*, 5405.
49. Valenta, J.; Juhasz, R.; Linnros, J. Photoluminescence Spectroscopy of Single Silicon Quantum Dots. *Appl. Phys. Lett.* **2002**, *80*, 1070.
50. Martin, J.; Cichos, F.; Huisken, F.; von Borczyskowski, C. Electron−Phonon Coupling and Localization of Excitons in Single Silicon Nanocrystals. *Nano Lett.* **2008**, *8*, 656.
51. Wang, X.; Ren, X.; Kahen, K.; Hahn, M.; Rajeswaran, M.; Maccagnano-Zacher, S.; Silcox, J.; Cragg, G.; Efros, A.; Krauss, T. Non-Blinking Semiconductor Nanocrystals. *Nature* **2009**, *459*, 686.
52. The double-peak structure can be viewed as slightly controversial since it was reported by some[50] but not by others,[26,29] and sometimes it was observed only in some[48] of the 1-nc spectra.
53. Note also that both our spectrum and the spectrum by Martin *et al.*[50] in Figure 6 exhibit a distinct indication of a third peak (second low-energy satellite), probably due to better signal-to-noise ratio.
54. Interestingly, we observe a small FTIR peak, whose origin we are not yet able to assign, exactly at this position.
55. Special capping in those nanocrystals consisted of replacing the usual abruptly changing confinement potential of core/shell CdZnSe/ZnSe nanocrystals with a shell formed by a radially graded alloy of CdZnSe into ZnSe in order to suppress Auger recombination mechanism.
56. Moskalenko, A. S.; Berakdar, J.; Prokofiev, A. A.; Yassievich, I. N. Single-Particle States in Spherical Si/SiO_2 Quantum Dots. *Phys. Rev. B* **2007**, *76*, 085427.
57. Sykora, M.; Mangolini, L.; Schaller, R. D.; Kortshagen, U.; Jurbergs, D.; Klimov, V. I. Size-Dependent Intrinsic Radiative Decay Rates of Silicon Nanocrystals at Large Confinement Energies. *Phys. Rev. Lett.* **2008**, *100*, 067401.
58. JCPDS PDF-2 release 2001, ICDD Newton Square, PA, USA.
59. Jerschow, A.; Muller, N. Convection Compensation in Gradient Enhanced Nuclear Magnetic Resonance Spectroscopy. *J. Magn. Reson.* **1998**, *132*, 13.
60. Kůsová, K.; Cibulka, O.; Dohnalová, K.; Pelant, I.; Matějka, P.; Žídek, K.; Valenta, J.; Trojánek, F. Colloidal Solution of Organically Capped Si Nanocrystals in Xylene: Efficient Photoluminescence in the Yellow Region *Mater. Res. Soc. Symp. Proc.* 2009 In *Applications of Group IV Semiconductor Nanostructures*; van Buuren, T., Tsybeskov, L., Fukatsu, S., Dal Negro, L., Gourbilleau, F., Eds.; Warrendale, PA, 2009; Vol. 1145E, 1145-MM04-13.